ACS OMEGA

http://pubs.acs.org/journal/acsodf

Article

The Influence of Specific Ions and Oxyhydroxo Species in Plant Water on the Bubble−Particle Attachment of Pyrrhotite

Lisa Louise October, Malibongwe Shadrach Manono,* Kirsten Claire Corin, Nora Schreithofer, and Jenny Gael Wiese

Cite This: *ACS Omega* 2021, 6, 28496−28506

Read Online

ACCESS | Metrics & More | Article Recommendations

ABSTRACT: Previous studies have considered the effect of using recycled process water in froth flotation and whether certain ions are responsible for what is observed in the final concentrate in terms of mineral grades and recoveries. The attachment of mineral particles to air bubbles is a fundamental subprocess of flotation, without which separation of valuable minerals from nonvaluables cannot occur; it is, therefore, of interest to assess the effect of specific ionic species on bubble−particle attachment. The effects of oxyhydroxo species on bubble−particle interactions were studied with three synthetic plant water (SPWs) of increasing ionic strengths at pH 11 as it is known to through solution speciation that at this pH, oxyhydroxo species may be present in significant concentrations. The presence of these oxyhydroxo species such as magnesium and calcium hydroxides in alkaline pulps were confirmed by many researchers and proven to affect bubble and particle surface charges. Furthermore, to ascertain whether there were certain ions within the plant water that impacted the bubble−particle attachment more significantly than others, tests were carried out with carefully selected single salt solutions. The SPWs at pH 11 resulted in very poor pyrrhotite attachment probabilities and recoveries as compared to the attachment probabilities and recoveries that were obtained with these waters at pH 6.5. Increasing the ionic strength of SPWs resulted in a decrease in pyrrhotite attachment probabilities more evidently at pH 11. Thus, it can be concluded that the presence of $CaOH^+$, $(MgOH)_2$, and $MgOH^+$ species hinders the flotation of pyrrhotite particles. Studies on selected single salts showed that Na^+ resulted in better pyrrhotite attachment probability and recovery compared to Ca^{2+}. Furthermore, upon studying the anion effect, SO_4^{2-} performed better than NO_3^- when paired with Ca^{2+}, thus indicating a negative effect on flotation response when Ca^{2+} and NO_3^- ions are used together. These results can be attributed to the action of species such as Ca^{2+}, $CaNO_3^+$, and $CaSO_4$(aq.) on the zeta potential and their consequential effect on the electrical double layer. The outcomes of this work should be of significant importance for an effective management of ions in recycled process water in the froth flotation process.

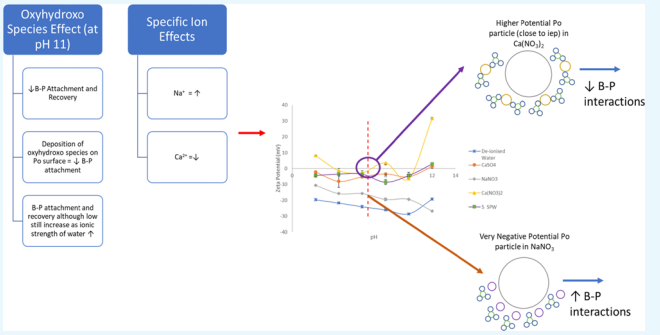

1. INTRODUCTION

In froth flotation, the selective separation between hydrophilic and hydrophobic particles is determined by the bubble−particle attachment subprocess. This subprocess of flotation is facilitated by interactions at the air−water and solid−water interfaces. Thus, this fundamental bubble−particle subprocess ultimately plays an important part in the recovery of valuable particles.

The bubble−particle attachment subprocess has been described in three steps by Albijanic et al.; the first step consists of the bubble approaching the particle, a film then forms at the solid−water and air−water interfaces. This film thins to critical thickness as the bubble and particle approach each other more closely. In the second step, when the bubble and particle are even closer in contact, the film becomes unstable and ruptures, resulting in the formation of a three-phase contact line, and bubble−particle attachment occurs. The third step consists of the bubble−particle contact line spreading across the surface, forming a stable wetting perimeter with equilibrium contact angles.[1]

Although the flotation process is critical in mineral processing operations for the recovery of valuable mineral particles, it can be quite water-intensive as the pulp in flotation cells consists of 80−85% water by volume.[2] Current fresh-water scarcities have, however, resulted in stringent environ-

Received: March 3, 2021
Accepted: June 23, 2021
Published: October 18, 2021

mental restrictions, resulting in many flotation plants seeking alternatives such as recycled and saline water. These water types do, however, contain high concentrations of electrolytes, and the difference in water chemistry between fresh water and recycled water may negatively affect the separation efficiency of the overall flotation process;[3] for example, the collector adsorption subprocess may be affected because of the surface-active nature of inorganic electrolytes on negatively charged surfaces.[4] Thus, the interactions between the water molecules and the mineral surface and between the water molecules and the electrical double layer at the mineral−water interface are important to consider, particularly in the presence of inorganic electrolytes.[5,6]

In electrolyte solutions containing bubbles and particles, both the double layers interact, resulting in double-layer repulsions. For successful bubble−particle attachment, the repulsion must be overcome with attractive forces and kinetic energy; thus, the double-layer repulsions behave as an energy barrier. It has been proposed that upon the addition of electrolytes, the electrical double layer compresses, reducing the energy barrier for bubble−particle attachment to occur.[7−10] The compression of the electrical double layer has been said to accelerate the rupture of the film at the air−water and solid−water interfaces, which, in turn, aids bubble−particle attachment.[10−12]

In the presence of inorganic electrolytes, the water structure may still be very strongly hydrogen-bonded; in this case, the ions are "structure making" because they retain the strong hydrogen bonds. These ions are small ions such as Na^+, Li^+, Mg^{2+}, F^-, and Cl^-, and they are of high surface charge density; therefore, structure makers are strongly hydrated and increase the viscosity of the solution.[13] In contrast to structure-making ions, the ions that tend to destroy the strongly hydrogen-bonded structure of water are known as "structure breakers." These are large ions such as Cs^+ and I^- and are weakly hydrated; these ions also tend to decrease the viscosity of the solution.[13−15]

Manono et al.[16] studied the effect of various single salts on copper and nickel recoveries. They showed no significant anion effect in terms of copper and nickel recoveries but did observe slightly higher recoveries with Na^+ from a cation perspective. This study by Manono et al.[16] maintained the ionic strength of various single salt solutions constant at 0.0213 M. This ionic strength could possibly be very low to see the effect of specific ions on mineral recoveries as the ionic strength of plant water used on a concentrator was shown to be closer to 0.0723 and 0.1205 M.[17] Following Manono et al.,[16] oxyhydroxo species were considered on a similar sulfidic copper and nickel ore in a different study;[18] it was shown that operating at pH 11 resulted in a decrease in copper and nickel recoveries, suggesting that the floatabilities of copper (chalcopyrite) and nickel (pentlandite) were impeded.

As this study specifically considers the bubble−particle attachment of pyrrhotite in specific inorganic electrolytes found in process water, building on the work of Manono et al.,[16,18] it was speculated that pyrrhotite would be of interesting consideration owing to its rather peculiar surface chemistry. A number of studies on the behavior and floatability of pyrrhotite against different pulp chemistry have been conducted.[19−30] It is important to note that pyrrhotite is an iron sulfide mineral with the formula $Fe_{(1-x)}S$, where $0 < x \leq 0.125$; this results in many pyrrhotite superstructures. At room temperature, four naturally occurring superstructures are known to exist and are divided into two categories, namely, magnetic monoclinic (Fe_7S_8 (4C)) and nonmagnetic hexagonal [Fe_9S_{10} (5C), $Fe_{10}S_{11}$ (11C), and $Fe_{11}S_{12}$ (6C)]. Both the flotation and depression of this pyrrhotite are a key operational driver in many flotation plants around the world, depending on the ore being processed.[31] For this reason, there has been interest to investigate various pyrrhotite structures under varying conditions.[25,32] These superstructures are known to result in different flotation responses as well as varying collector adsorption. Nonmagnetic hexagon pyrrhotite (5C) has shown to be more floatable than magnetic monoclinic pyrrhotite (4C).[19] Studies by Multani et al.[27−30] showed better xanthate adsorption with magnetic pyrrhotite compared to that with its nonmagnetic counterpart, although lower recovery was seen with the magnetic pyrrhotite. This led the authors to hypothesize that different dixanthanogen amounts may exist in various superstructures and that nonmagnetic pyrrhotite contains more dixanthogen. Impedance values were shown to be significantly higher at pH 10 for all pyrrhotite samples used in a study by Ekmekci et al.[26] because of higher oxidation that exists in alkaline solutions. The authors further showed that the addition of xanthate does not affect the recovery at pH 10 because of the low rate of dixanthogen formation with alkaline solutions, thus resulting in lower recoveries compared to their results at pH 7.

A previous study by October et al.[33] showed the effect of increasing ionic strength of synthetic plant water (SPW) on the bubble−particle attachment of pyrrhotite. This study showed decreased xanthate adsorption on the pyrrhotite surface as the ionic strength of the plant water increased, and this resulted in a decrease in attachment probability as the water quality deteriorated. It may be that it is a specific ion that is responsible for this result, and if this is the case, the removal of this ion will be a more cost-effective and environmentally friendly exercise compared to treating the water or bringing in fresh water. October et al.[33] further showed that the potential of pyrrhotite tends to increase with increasing ionic strength, indicating possible adsorption of the specific metal cations on the mineral. The zeta potential results by the same study showed that across all water types, a distinct increase in potential occurred between pH 10 and 12. Studies by Rao and Finch[34] and Zanin et al.[35] showed that hydrophilic $CaOH^+$ species, as with other polyvalent metal cations, adsorb onto the surfaces of sulfide minerals, resulting in a reversal in the zeta potential of the sulfide mineral surface. Furthermore, Li et al.[36] confirmed via X-ray photoelectron spectroscopy (XPS) studies the adsorption of $(MgOH)_2$ on the chalcopyrite surface in $MgCl_2$ solution at pH 10. They also showed how the pH, at which $(MgOH)_2$ precipitation occurred, becomes lower than pH 10 as the concentration of $MgCl_2$ is increased, which is in line with the work of Li and Somasundaran.[37] Ramos et al.[38] reported that the charge of the bubble should be assessed when cationic hydroxyl complexes are formed in flotation pulps because of the high pH of the pulp. Li and Somasundaran[37] also reported that magnesium hydroxyl and other hydroxide complexes were approaching the liquid−air interface, which resulted in a positive charge on the bubble surface. It is thus evident that magnesium hydroxyl and other hydroxide complexes coat the mineral surface at alkaline pulp conditions, resulting in both a more positive bubble and particle. This effect on the charge of the bubble and particle is expected to affect the bubble−particle attachment efficiency. A more recent study by October et al.[33] showed increases in the zeta potential

https://doi.org/10.1021/acsomega.1c01152
ACS Omega 2021, 6, 28496−28506

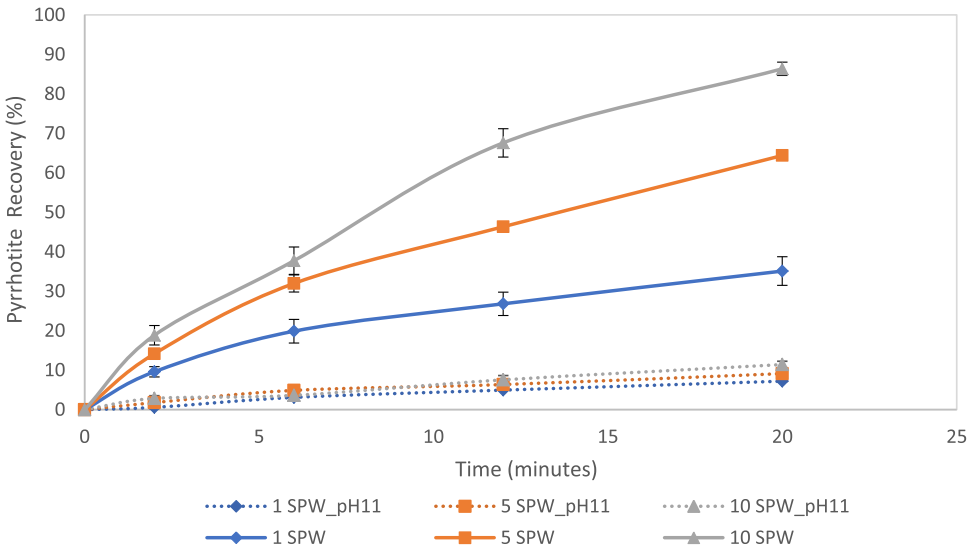

Figure 1. Microflotation of pyrrhotite under varying water quality at natural pH and pH 11 (error bars represent standard error of the mean).

of pyrrhotite between pH 10 and pH 12; therefore, such increases were attributed to the formation of the oxyhydroxo species in the SPW at alkaline conditions.

Furthermore, a study into ion−reagent−mineral interactions in flotation by Manono et al.[39] showed that SPWs of increasing ionic strengths at pH greater than 10 exhibited increased concentrations of oxyhydroxo species. The presence of these oxyhydroxo species in plant water may affect bubble−particle attachment; thus, it is of interest to assess the impact that these oxyhydroxo species would have on the bubble−particle attachment of pyrrhotite. Furthermore, it is of interest to determine if there are specific ions in plant water that are either beneficial, detrimental, or have no effect on the bubble−particle attachment subprocess and subsequently on the overall flotation process.

2. RESULTS AND DISCUSSION

2.1. Oxyhydroxo Species in SPW on the Bubble−Particle Attachment of Pyrrhotite. Bubble−particle interactions were studied both from a fundamental and microflotation perspective to assess the effect of the presence of the oxyhydroxo species in SPW. Studies by Manono et al.[39] observed the existence of these species in SPW with pH greater than 10.

Figure 1 shows the microflotation results of SPW at pH 6.5 and pH 11. Figure 1 clearly shows that much more pyrrhotite is recovered at the natural pH and that recoveries at pH 11 are extremely low across all three water qualities. The recovery of pyrrhotite is shown to increase significantly as the ionic strength of the plant water increases at the natural pH. While the recovery of pyrrhotite at pH 11 does not show a discernable difference across the varying water qualities, it should, however, be noted that the recovery at pH 11 with 1 SPW is slightly less than that with 10 SPW. It is evident from Figure 1 that despite the presence of a xanthate collector, which should endow the sulfide mineral with sufficient hydrophobicity, the increase in pH from natural pH to pH 11 hinders the recovery of the mineral. Speciation diagrams of the SPWs published by Manono et al.[39] showed that at pH 11, there existed oxyhydroxo species that were not present at pH 6.5. The decrease in pyrrhotite recovery at pH 11 is attributed to the presence of these oxyhydroxo species as these are known to have a depressive effect on pyrrhotite.[31] The effect of these oxyhydroxo species is further reinforced by the surface charge of pyrrhotite. October et al.[33] showed that for a fixed ionic strength of SPW, the zeta potential of pyrrhotite increases distinctly at around pH 11 to a more positive potential. Therefore, the trend in the potential of pyrrhotite at more alkaline pH values is attributed to the formation and deposition of these oxyhydroxo species on the pyrrhotite surface, not only preventing its flotation but, in turn, also preventing processes such as collector adsorption and the compression of the electrical double layer from taking place. However, it needs to be stated that this proposed mechanism, which considers electrostatically driven rupture of the wetting film, supported by the findings of this work, is mostly valid for sufficiently hydrophilic particles, among which pyrrhotite's natural hydrophobicity is negatively affected in ionic solutions containing Ca^{2+} and its oxyhydroxo species; for hydrophobic particles, nucleation mechanisms may prevail and the bubble and mineral surface charge may prove to be of minor importance.[40−42] Thus, future work, considering the contact angle vs xanthate concentration under different inorganic electrolytes concentrations, would be needed to decouple these mechanisms.

Figure 2 shows a comparison of the zeta potential of pyrrhotite at pH 6.5 (natural pH) and pH 11 for all three SPWs tested. It is clear that the potential of pyrrhotite is less negative at pH 11 compared to that at pH 6.5 and that a trend of an increase in the potential of the mineral surface is seen with an increase in the ionic strength. The speculation of the presence of oxyhydroxo species at pH 11 in increasing ionic strengths of plant waters is supported by speciation diagrams that are presented in the study by Manono et al.,[39] which showed clear trends of increases in the concentration of the oxyhydroxo species at pH > 9. This oxyhydroxo species were shown to be in the form of species such as $Mg(OH)^+$, $CaSO_4$(aq.), and $Ca(OH)^+$ among others and are reported elsewhere as being passivating and have the potential to form slimes and coatings on mineral surfaces.[43]

Under the same conditions as the microflotation tests, the automated contact time apparatus (ACTA) was used to study the effect of the presence of oxyhydroxo species in SPW on bubble−particle attachment from a fundamental level. Figure 3

https://doi.org/10.1021/acsomega.1c01152
ACS Omega 2021, 6, 28496−28506

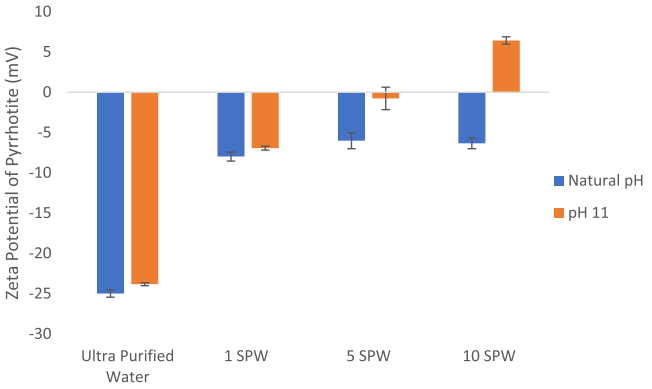

Figure 2. Zeta potential of pyrrhotite under varying water quality at the natural pH (pH 6.5) and pH 11 (error bars represent the standard error of the mean).

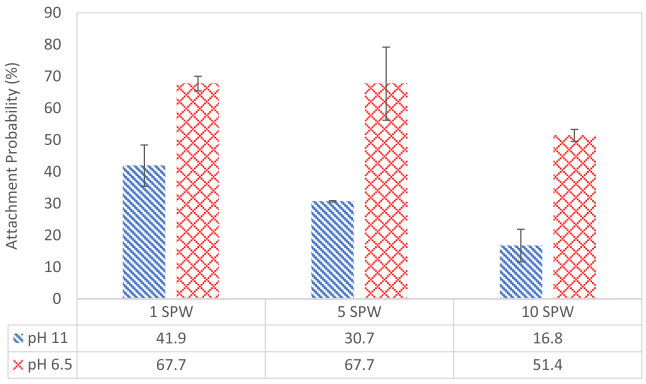

Figure 3. Attachment probability of pyrrhotite under varying water quality at the natural pH and pH 11

presents the attachment probability of pyrrhotite at an increasing ionic strength at the natural pH (as per October et al.[33]) as well as the attachment probability with these SPW types at pH 11.

The attachment probability at the natural pH, as reported by October et al.,[33] showed a decrease in the attachment probability with an increase in the ionic strength of the plant water. It needs to be noted that this trend is directly opposite of what is seen in the microflotation recoveries of pyrrhotite. This behavior may be due to the varying operating conditions in the two equipment (ACTA and microflotation cell). Although this is the case, it is evident that even from a fundamental level, substantially less particles attach to air bubbles at pH 11, as seen with the drop in the attachment probability at pH 11 compared to the natural pH results. Thus, a possible deposition of the oxyhydroxo species on the pyrrhotite surface may have induced the hydrophilicity of pyrrhotite particles.

Studies have shown that the adsorption of cations on the mineral surface not only changes the surface charge of the minerals but also results in the formation of hydrophilic agglomerates.[39,44] The zeta potential measurements shown in Figure 2, which were generated under the chemical conditions shown in Figures 1 and 3, show that between pH 9 and 12, either the isoelectric point is reached or the potential of the pyrrhotite is close to 0 mV. This is well explained in a previous study by October et al,[33] and a previous study has shown that at 0 mV, the particles tend to agglomerate;[13] given that the oxyhydroxo species exist at this pH range,[39] the agglomeration of pyrrhotite particles with the oxyhydroxo species at its surface may result in substantial pyrrhotite depression, as seen in Figures 1 and 3.

2.2. Specific Ions on the Bubble−Particle Attachment of Pyrrhotite. In order to further understand the effects of specific ionic species within plant water, it was deemed necessary to determine if there are single ions in plant water that are either beneficial, detrimental, or have no effect on the bubble−particle attachment subprocess.

The microflotation test results in single salt solutions are presented in Figure 4. Figure 4 shows that the $NaNO_3$ solution

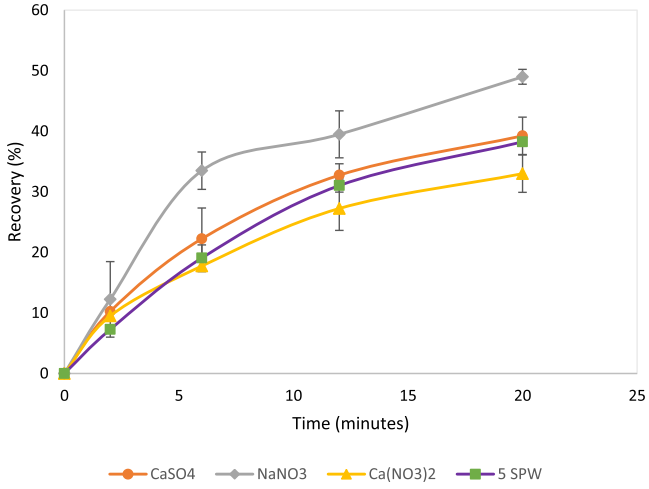

Figure 4. Microflotation recovery of pyrrhotite in various solutions at the natural pH (error bars represent the standard error of the mean).

resulted in the highest recovery of pyrrhotite at 49.0%, followed by the $CaSO_4$ solution at 39.0% recovery, while the lowest recovery was obtained with the $Ca(NO_3)_2$ solution with 33.0% of pyrrhotite recovered. The final recovery of pyrrhotite using SPW at the same ionic strength of these single salt solutions was found to be 36.5%.

The microflotation results show that the Ca salts resulted in lower recoveries of pyrrhotite compared to that of the Na salts. Studies have shown that in single salt solutions at higher ionic strengths, the hydration layer stability decreases.[13,36] Hirajima et al.[45] noted longer induction times and subsequent decreases in recovery to be due to increases in the stability of the hydration layer. Therefore, it can be inferred that in the Na^+ solution, the hydration layer stability decreases, making the time for the bubble and particle to attach shorter. This finding is in agreement with that of Blake and Kitchener,[46] who reported that stable films of hydration layers are reduced in Na^+ solutions. The reduction in the hydration layer stability leads to the compression of the electrical double layer around mineral particles, and as a result, this leads to an opening of hydrophobic particle surface sites, attracting air bubbles by hydrophobic bonding. Li[36] also proposed that the addition of certain inorganic electrolytes decreased the energy barrier in wetting film rupture by compressing the electrostatic double-layer force and thereby improved bubble−particle attachment. In contrast, other studies by Craig et al.[47] and Paulson and Pugh[7] propose that floatability is increased with electrolytes of higher valency. Although this is not the case with the Ca^{2+} cation, the SO_4^{2-} anion does outperform its NO_3^- counterpart when paired with the Ca^{2+} cation in the microflotation tests.

https://doi.org/10.1021/acsomega.1c01152
ACS Omega 2021, 6, 28496−28506

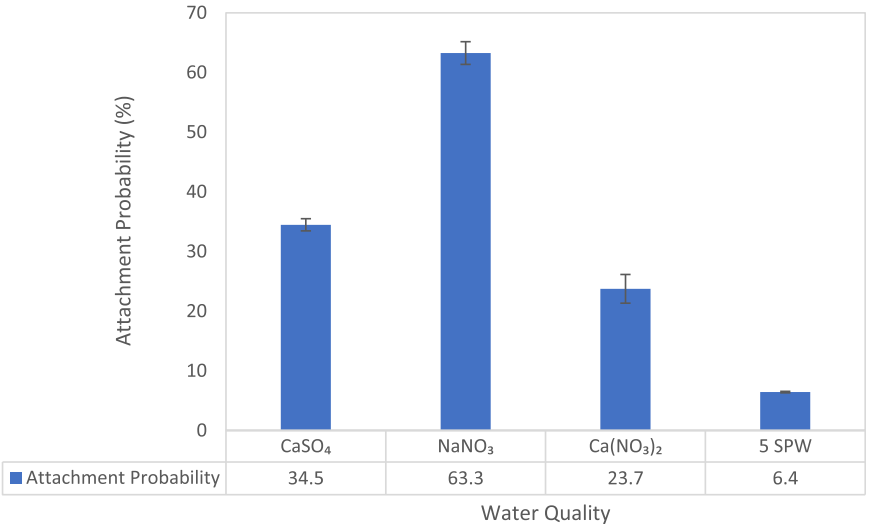

Figure 5. Attachment probability of pyrrhotite in various solutions at the natural pH (error bars represent the standard error of the mean).

The attachment timer results presented in Figure 5 give an account of the effect of $CaSO_4$, $NaNO_3$, $Ca(NO_3)_2$, and SPW (5 SPW) on the bubble−particle attachment probability of pyrrhotite particles to air bubbles from a fundamental bubble−particle attachment perspective.

The highest probability of attachment in the single salt solutions was achieved in the $NaNO_3$ solution, followed by $CaSO_4$, while the lowest attachment probability was achieved with the $Ca(NO_3)_2$ single salt solution. The SPW of the same ionic strength as the three single salt solutions yielded a considerably lower attachment probability compared to that of the single salt solutions, which could be due to the combined effect of various ions present in the SPW. This may also be due to the fact that the concentrations of the anions and cations in the single salt solutions are higher than the concentration of the particular cation and anion of interest in the SPW matrix, although the total ionic strength is the same as shown in Table 1. The trend observed with the single salt solutions indicates

Table 1. Mineralogical Composition of Pyrrhotite

sulfide mineral	XRD results	
pyrrhotite	mineral	composition (weight %)
	quartz	4.20
	sphalerite	2.56
	chalcopyrite	1.62
	pyrrhotite 5C	91.62

that the Na^+ cation generally results in a higher attachment probability compared to the Ca^{2+} cation. This may be due to a monovalent versus divalent effect in how these types of ions passivate the mineral surface. It is expected that this effect should become clearer upon studying the effect of these ions on the zeta potential of the mineral.

2.3. Specific Ions on the Zeta Potential of Pyrrhotite in Single Salt Solutions. Figure 6 shows the zeta potential measurements of the three salt solutions and SPW over the pH range of 2−12, all at the same ionic strength of 0.1205 M. The dashed line in Figure 6 indicates the pH at which the microflotation and attachment time tests for these solutions were conducted. Also, the speciation diagrams of the three salts under investigation are indicated in Figure 7 over the pH range 2−12. Figure 6 illustrates that the zeta potentials of pyrrhotite in the salt solutions are generally less negative than those in deionized water over the pH range studied, indicating the adsorption of metal cations on the mineral surface.[48] $Ca(NO_3)_2$, $CaSO_4$, and SPW result in a much more positive potential on the pyrrhotite surface compared to the deionized water and $NaNO_3$ solution, which lead to a more negative pyrrhotite surface. Because of the small, strongly hydrated nature of Na^+, it is expected that it will result in the preservation of the strongly hydrogen-bonded water structure and increase the viscosity of the solution.[15] It has also been shown that with an increase in the magnitude of particle potential, the viscosity increases.[49] This work, therefore, confirms that the zeta potential of pyrrhotite is strongly negative in the Na^+ than the other salt solutions, and this may be due to the effect that valency (monovalent vs divalent) has on the viscosity, and hence, a higher viscosity of the Na^+ solution compared to that of the Ca^{2+} solutions may be the reason for the differences seen.

Evidently, the Ca^{2+}-containing solutions result in a stronger passivation of the pyrrhotite surface. This result is similar to that achieved by Harvey et al.[10] in coal flotation studies. They showed that the magnitude of the zeta potential depended on the valency of the cation, with the divalent Mg^{2+} providing a greater increase in the zeta potential compared to the monovalent Na^+. This result is in line with the results in this work, whereby Ca^{2+} passivated the pyrrhotite surface more than Na^+, as seen by the more positive potential in the Ca^{2+} solution.

Furthermore, upon studying the anion effect, the $CaSO_4$ solution resulted in a lower (more negative) zeta potential than the $Ca(NO_3)_2$ solution. Evidently, the cation type played a significant role in the charge of the pyrrhotite surface; when the NO_3^- anion is paired with the monovalent cation, the pyrrhotite potential is approximately 19 mV lower than that when paired with the divalent Ca^{2+} cation. On average, the $Ca(NO_3)_2$ solution resulted in higher pyrrhotite potential compared to the other Ca^{2+}-containing solutions; thus, the combination of Ca^{2+} and NO_3^- ions results in higher pyrrhotite potentials.

Figure 7 illustrates the speciation of the solutions under study, as generated by Visual MINTEQ. Figure 7(a) shows the speciation of the $CaSO_4$ solution at an ionic strength of 0.1205

https://doi.org/10.1021/acsomega.1c01152
ACS Omega 2021, 6, 28496−28506

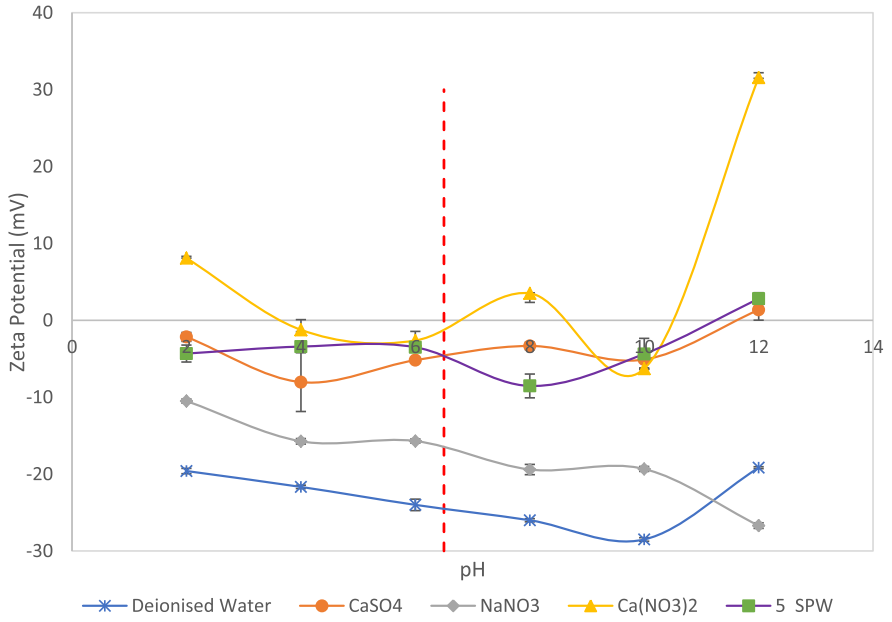

Figure 6. Zeta potential measurements of pyrrhotite as a function of pH in various solutions (error bars represent the standard error of the mean).

M. Below pH 4, the dominant species in the solution include HSO_4^-, H^+, $CaSO_4$ (aq.), SO_4^{2-}, and Ca^{2+}. Between pH 4 and 10, the concentration of H^+ drops close to 0 M. Beyond pH 10, a dramatic increase in OH^- is observed and further increases in $Ca(OH)^+$.

Figure 7(b) shows the speciation of the $Ca(NO_3)_2$ solution at an ionic strength of 0.1205 M. Below pH 4, the dominant species in the solution include NO_3^-, Ca^{2+}, H^+, and $CaNO_3^+$. Between pH 4 and 10, HSO_4^- and H^+ drop close to 0 M. Beyond pH 10, an increase in OH^- and $Ca(OH)^+$ concentrations is evident, whereas a decrease in Ca^{2+} is observed.

Figure 7(c) shows the speciation of the $NaNO_3$ solution at an ionic strength of 0.1205 M. Below pH 4, the dominant species in the solution include NO_3^-, Na^+, and H^+. Between pH 4 and 10, the concentration of H^+ drops close to 0 M; beyond pH 10, an increase in the OH^- concentration is observed; however, NO_3^- and Na^+ concentrations remain high.

Figure 7 clearly shows an increase in the metal hydroxide complexes between pH 10 and 12. Hydroxide precipitation or oxidation at the mineral surface may be a reason for the increase in the potential in various salt solutions at pH 10 to 12, as observed in Figure 6.[10,45,50]

Relating both the attachment time and microflotation tests to the zeta potential measurements, a cation and anion effect is observed. The pyrrhotite recovery and bubble−particle attachment are greater with the $NaNO_3$ solution than with the $Ca(NO_3)_2$ solution, while the zeta potential measurements confirm an increase in the zeta potential with $Ca(NO_3)_2$. From an anion perspective, SO_4^{2-} performs better than NO_3^- when paired with Ca^{2+}.

Although the mechanism is not completely clear, previous studies have also shown that divalent anions such as SO_4^{2-} and $S_2O_3^{2-}$ improve the flotation efficiency.[16,51] Furthermore, it should be noted that although conducted at the same ionic strength, the Ca^{2+} concentration is higher in $Ca(NO_3)_2$ compared to $CaSO_4$; as a result, this may possibly show the dominant effect of Ca^{2+} overpowering any anion effect that may exist.

The zeta potential measurements also verify a much more negative pyrrhotite surface potential with the $NaNO_3$ solution. As previously stated, increases in ionic strength compress the electrical double layer, reducing the energy barrier for bubble−particle attachment to occur.[7,9,10] Thus, with a highly negative zeta potential as in the $NaNO_3$ solution, it is expected that the high repulsion between the particle and bubble would result in a higher energy barrier, leading to decreased recoveries. This was not evidently observed, indicating that another mechanism may be resulting in the higher recoveries and attachment probabilities with monovalent salt solutions. As previously described, the monovalent solution may result in decreased hydration layer stability, resulting in a more rapid bubble−particle attachment. Another possibility could be the effect of the changes in the zeta potential of the bubble with the $NaNO_3$ solution; this may result in an optimal bubble−particle attachment if the charge of the bubble becomes positive enough such that the energy barrier for attachment is decreased. A study has been performed by Takahashi[52] focusing on the charge of the bubble, and as with the particle, higher-valency cations do make the surface charge of the bubble less negative. This study was, however, performed with the bubble in isolation and did not consider the particle.

It is important to mention that another mechanism, which could be important to consider, is related to the effects of inorganic electrolytes on bubble coalescence, affecting the bubble size, which would in turn affect the bubble surface area on which bubble−particle contact occurs. A study by Lessard and Zieminski[62] showed that multivalent cations and anions have a greater ability to inhibit bubble coalescence, while Craig[63] reported that solutions containing single salts of $NaNO_3$ and $Ca(NO_3)_2$ inhibited bubble coalescence; this, in turn, resulted in small bubble diameters. It is also well known that high concentrations of electrolytes, as with frothers, have bubble-size-reducing ability.[53,54] Although in this study, the total ionic strength was maintained constant at 0.1205 M for all salt solutions, the $NaNO_3$ solution exhibited a higher molarity

https://doi.org/10.1021/acsomega.1c01152
ACS Omega 2021, 6, 28496−28506

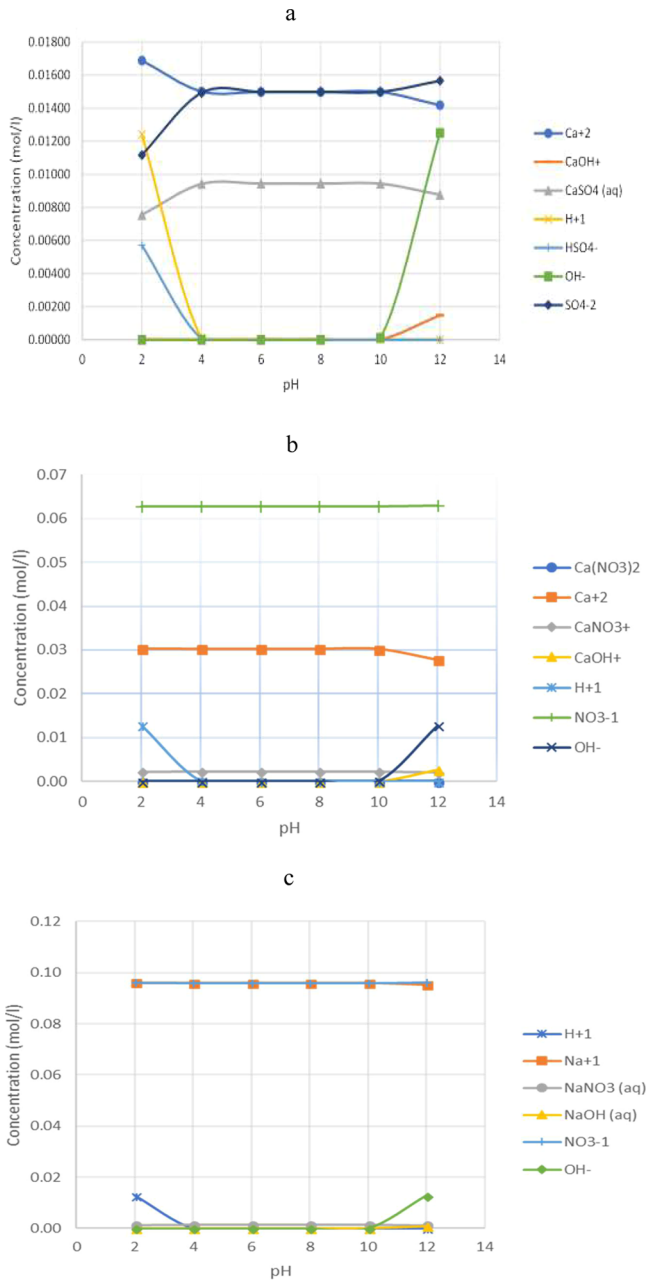

Figure 7. Speciation diagrams of (a) $CaSO_4$, (b) $Ca(NO_3)_2$, and (c) $NaNO_3$.

of 0.1205 M compared to $Ca(NO_3)_2$ and $CaSO_4$, which exhibited molarities of 0.0402 and 0.0301 M, respectively. Manono et al.[55] used the same salt solutions at a five times lower ionic strength and showed that the mean bubble diameter in the $NaNO_3$ solution was 1.55 mm; this was slightly larger compared to that of $Ca(NO_3)_2$ (1.28 mm) and $CaSO_4$ (1.31 mm), as expected in that the monovalent Na^+ would typically be less effective in retarding bubble coalescence compared to the divalent Ca^{2+}. Thus, in the $NaNO_3$ solution, the results of a higher attachment probability and microflotation recovery compared to the results with the solutions of $Ca(NO_3)_2$ and $CaSO_4$ would be counterintuitive if bubble-size effects were considered alone without considering the effects of these inorganic electrolytes on solution chemistry and pyrrhotite chemistry. Therefore, the findings of this study concerning single salt solutions, as reported in Figures 4567, point to the effects of Ca^{2+} and its oxyhydroxo species on the surface chemistry of pyrrhotite and their resulting impact on the hydrophobicity and floatability of pyrrhotite. Thus, the more positive pyrrhotite zeta potential in Ca^{2+} points to a more passivated surface that could have induced a more hydrophilic nature on pyrrhotite and hence the lower recoveries and attachment probabilities reported in the presence of Ca^{2+}.

3. CONCLUSIONS

Thus, the following conclusions have been made from the findings of this study:

- Plant water at pH 11 results in low bubble−particle interactions across various water qualities even in the presence of a collector because of the deposition of oxyhydroxo species on the pyrrhotite surface, as suggested by increased pyrrhotite potentials.[33]
- Monovalent cations and divalent anions result in greater bubble−particle attachment. The fact that monovalent cations outperformed divalent cations calls for the investigation of properties such as viscosity in monovalent solutions and how these mechanistically affect the hydration-layer stability. Furthermore, the zeta potential of the bubbles generated in various solutions could add more value to this area of research if studied alongside the zeta potential of the mineral.
- Poor recoveries and attachment probabilities of pyrrhotite in various plant waters at pH 11 are attributed to the deposition of oxyhydroxo species such as $CaOH^+$ and $MgOH^+$ on the pyrrhotite surface, which were shown to exist at pH > 10 in a study by Manono et al.[39] The formation of these oxyhydroxo species was confirmed by the following authors: Rao and Finch,[34] Zanin et al.,[35] Li et al.,[36] Li and Somasundaran,[37] and Ramos et al.[38]
- The outcomes of this work suggest that not only do these species prevent the flotation of the mineral particles but, in turn, they also prevent processes such as collector adsorption and compression of the electrical double layer from taking place.
- A clear anion and cation effect was observed in the attachment time and microflotation tests, and these were supported by zeta potential measurements. The attachment time and microflotation tests showed that $NaNO_3$ exhibited the highest bubble−particle attachment probability and pyrrhotite recovery, respectively, while the $Ca(NO_3)_2$ solution resulted in the poorest performance. The sulfate anion was shown to be more beneficial to the floatability of pyrrhotite compared to the nitrate anion when paired with divalent cations.
- The $NaNO_3$ solution led to an increased performance compared to $Ca(NO_3)_2$, as confirmed by the attachment time and microflotation tests. Upon studying the potential of pyrrhotite with these two nitrate salts, a considerably lower charge with $NaNO_3$ was observed compared to that with pyrrhotite in the $Ca(NO_3)_2$ solution, indicating the effect that the Ca cation has in increasing the potential of pyrrhotite.

4. MATERIALS AND METHODS

4.1. Mineral Sample. Pyrrhotite (1 kg), obtained from Ward's Science, was crushed to 100%-passing 1000 μm with a hammer; the crushed particles were pulverized and screened

https://doi.org/10.1021/acsomega.1c01152
ACS Omega 2021, 6, 28496−28506

Table 2. Concentrations of Ions for the Various SPW and Single Salt Solutions

plant water type	Ca^{2+} (mg/L)	Mg^{2+} (mg/L)	Na^{+} (mg/L)	Cl^{-} (mg/L)	SO_4^{2-} (mg/L)	NO_3^{-} (mg/L)	CO_3^{2-} (mg/L)	TDS (mg/L)	ionic strength (IS) (mol/L)
1 SPW	80	70	153	287	240	176	17	1023	0.0241
5 SPW	400	350	765	1435	1200	880	85	5115	0.1205
10 SPW	800	700	1530	2870	2400	1760	170	10,230	0.241
$Ca(NO_3)_2$	1610					4981		6591	0.1205
$CaSO_4$	1207				2894			4101	0.1205
$NaNO_3$			2770			7472		10,242	0.1205

(dry) to −75, +38, and − 25 μm fractions. A rotary splitter was used to split the sample in smaller representative samples; each of these samples were purged with nitrogen and refrigerated below −30 °C. The particle size fraction −75 and +38 μm was used for the attachment time and microflotation tests, while the −25 μm fraction was used for the zeta potential measurements; because for this measurement, particles must be fine enough such that some particles are still suspended in the solution. Table 1 provides an account of the mineralogical compositions of pyrrhotite. Powder X-ray diffraction (PXRD) spectra were obtained using a Bruker D8 Advance powder diffractometer with a Vantec detector, fixed divergence, and receiving slits with Co-Kα radiation. The phases were identified using the Bruker Topas 4.1 software, and the relative phase amounts (weight %) were estimated using the Rietveld method.

4.2. Water Quality. SPW of ionic strength 0.0241 M, as described by Wiese et al.[56] was used in this study. However, it is acknowledged that because of onsite water recirculation that may cause increases in the ionic strength and total dissolved solids in process water, the quality of water within sulfide concentrators may have changed substantially; hence, studies conducted within the Centre for Minerals Research at the University of Cape Town have spiked the ion concentrations and total ionic strengths of synthetically prepared plant water.[57,58] Therefore, for this study, in order to simulate the recirculation of SPW, the amount of dissolved solids was increased by 5 and 10 times. These plant water solutions are referred to as 5 SPW (0.1205 M) and 10 SPW (0.241 M), respectively. Also, $NaNO_3$, $Ca(NO_3)_2$, and $CaSO_4$ single salt solutions with an ionic strength of 0.1205 M were prepared along with the SPW of the same ionic strength. Table 2 shows the ionic concentration of these prepared SPWs and single salt solutions. Where necessary, the pH of the SPW solutions was adjusted with 1% w/v solutions of NaOH and HCl.

The investigation studying the effect of an increase in the pH of the SPW was conducted in the presence of sodium isobutyl xanthate (SIBX) as a collector, as the study by October et al.[33] showed that the adsorption of the collector on pyrrhotite was affected by the water quality, and it subsequently affected bubble−particle interactions. In this way, the tests assessing bubble−particle interactions at the natural pH (pH 6.5) in the aforementioned study are directly compared to the work in this investigation at the adjusted pH (pH 11).

Upon considering specific-ion effects on the bubble−particle attachment of pyrrhotite, tests on single salt solutions were carried out in the absence of a collector. Single salt studies assessing bubble−particle interactions by Yoon and Yordan[59] showed that collector dosage may actually impact attachment time and overpower the effect of the ionic concentration. Therefore, as a starting point, the single salt work in this study is in the absence of a collector.

The salts used for the preparation of the SPWs were of analytical grade, while the SIBX was 97% purity. All salts were supplied by Merck, while the powdered form of SIBX was supplied by Senmin.

4.3. Attachment Time Tests. This investigation used the ACTA to measure bubble−particle interactions from a fundamental perspective. This instrument was developed at Aalto University and has been described in publications by Jávor et al.,[60,61] Aspiala et al.,[62] and October et al.[33]

The particle bed was prepared by first mixing 9 g of pyrrhotite with 100 mL of the particular water whose quality is under study. When a collector was utilized, the slurry was conditioned for 1 min with 100 g/t (standard industry dosage) SIBX; the slurry was allowed to settle, and the clear liquid was pipetted out and filtered until about 2 cm of the liquid remained above the settled particles. The filtrate was placed in the glass pool, after which the settled particles were pipetted into the pool for building the particle bed. Furthermore, to attain a flat particle bed of 2 mm, an automated shovel was employed. Measurements were taken for each of the water qualities, as shown in Table 3, and were performed in duplicate

Table 3. Properties of Deionized Water

resistivity at 25 °C (MΩ·cm)	conductivity (μs/cm)	total organic carbon (μg/L)	Na^{+} (μg/L)	Cl^{-} (μg/L)
18.2	<0.055	<5	<1	<1

for each condition. The slurry was adjusted to pH 11 in the investigation assessing the effect of an increase in pH; this was performed by means of NaOH. Tests on single salts were conducted at the natural pH, which was around 6.5. The temperature was recorded to be an average of 20 °C.

4.4. Microflotation Tests. The microflotation cell developed by Bradshaw and O'Connor[63] was used to perform the microflotation tests in this investigation. Pyrrhotite (3 g) was mixed with 50 mL of the water whose quality is under study. The mixture was then ultrasonicated for 5 min to remove oxidation products from the mineral surface and prevent particle agglomeration. The pyrrhotite−salt solution slurry was then dispersed into the microflotation cell. A constant air flow of 7 mL/min was introduced into the microflotation cell, and the peristaltic pump circulating the pulp was set to 90 rpm. For the tests with the collector (SPW solutions), a volume (20 μL) equivalent to 100 g/t of 1% SIBX solution was added to the cell and conditioned for 1 min. Four concentrates were collected, after 2, 6, 12, and 20 min. The concentrates and tails were filtered and dried. The microflotation tests were performed in duplicate for each SPW and single salt solution. Similar to the tests with the ACTA, the slurry was adjusted to pH 11 with NaOH, when pH 11 was

https://doi.org/10.1021/acsomega.1c01152
ACS Omega 2021, 6, 28496−28506

considered. The single salts tests were conducted at the natural pH (6.5), and the temperature was recorded to be an average of 20 °C. It needs to be stated that no frother was used in the microflotation experiments because microflotation tests conducted aimed at studying the interactions occurring in the pulp phase between the water borne ions and collector adsorption on the surface of pyrrhotite. The addition of a frother may result in additional interactions occurring, which is out of the scope of this study.

4.5. Zeta Potential Measurements. In a beaker, 60 mL of the single salt solution was mixed with 0.075 g of pyrrhotite particles. This dilute mixture was divided in six containers of equal volume. The pH of each container was adjusted using weak HCl and NaOH solutions to pH values of 2, 4, 6, 8, 10, and 12. Each container was labeled with the pH of its solution. Each solution was stirred for 15 min on a magnetic stirrer, after which the pH was measured again and, if necessary, readjusted.

The solution was allowed to settle; 1 mL of the top liquid was drawn (includes fine particles suspended in the liquid), inserted in the Malvern dip cell (Malvern Instruments Ltd., Malvern, UK), and placed in the Malvern ZetaSizer Nano ZS90 (Malvern Instruments Ltd., Malvern, UK), in which measurements were taken. All measurements were performed in triplicate to reduce experimental error. It is important to note that zeta potential measurements of pyrrhotite in SPWs of increasing ionic strengths over the pH range of 2−12 were previously published by October et al[33] The temperature at which these measurements were conducted was recorded to be an average of 20 °C.

4.6. Speciation of Single Salt Solutions. The concentration of the dominant species present in the single salt solutions over the pH range of 2−12 was calculated using Visual MINTEQ version 3.1. This tool uses thermodynamic equilibrium data to calculate ion speciation in water.[64] These calculations were considered at a fixed temperature of 20 °C.

AUTHOR INFORMATION

Corresponding Author

Malibongwe Shadrach Manono − *Centre for Minerals Research, Department of Chemical Engineering, University of Cape Town, Rondebosch 7701, South Africa;* orcid.org/0000-0002-2928-9368; Email: malibongwe.manono@uct.ac.za

Authors

Lisa Louise October − *Centre for Minerals Research, Department of Chemical Engineering, University of Cape Town, Rondebosch 7701, South Africa*

Kirsten Claire Corin − *Centre for Minerals Research, Department of Chemical Engineering, University of Cape Town, Rondebosch 7701, South Africa*

Nora Schreithofer − *Department of Bioproducts and Biosystems, Clean Technologies Research Group, Aalto University, Espoo 02150, Finland*

Jenny Gael Wiese − *Centre for Minerals Research, Department of Chemical Engineering, University of Cape Town, Rondebosch 7701, South Africa*

Complete contact information is available at: https://pubs.acs.org/10.1021/acsomega.1c01152

Notes

The authors declare no competing financial interest.

ACKNOWLEDGMENTS

This work is financed by the National Research Foundation of South Africa (NRF) [Grant number 103641] and the Academy of Finland (AF) as part of the joint project "Bridging North to South" in the MISU program. Any opinion, finding, conclusion, or recommendation expressed in this material is that of the authors', and the NRF does not accept any liability in this regard. Further, the financial and technical contributions from the South African Minerals to Metals Research Institute (SAMMRI) are also acknowledged.

REFERENCES

(1) Albijanic, B.; Ozdemir, O.; Nguyen, A. V.; Bradshaw, D. A Review of Induction and Attachment Times of Wetting Thin Films between Air Bubbles and Particles and Its Relevance in the Separation of Particles by Flotation. *Adv. Colloid Interface Sci.* **2010**, *159*, 1−21.

(2) Muzenda, E. An Investigation into the Effect of Water Quality on Flotation Performance. *World Academy of Science, Engineering and Technology* **2010**, *4*, 562−566.

(3) Slatter, K.A. ; Plint, N.D.; Cole, M.; Dilsook, V.; De Vaux, D.; Palm, N.; Oostendorp, B. *Water Management in Anglo Platinum Process Operations : Effects of Water Quality on Process Operations.* Abstracts of the International Mine Water Conference, South Africa, 19th − 23rd Oct. 2009 Proc. ISBN Number 978-0-9802623-5-3, 2009, No. October, 46−55.

(4) Yoon, R.H.; Basilio, C. I. Adsorption of Thiol Collectors on Sulphide Minerals and Precious Metals: A New Perspective. In *XVIII International Mineral Processing Congress*; 1993; 611−618.

(5) Fuerstenau, D W; Mishra, R. K. On the Mechanism of Pyrite Flotation with Xanthate Collectors. In *Complex Sulfides*; Jones, M. H., Ed.; Institute of Mining and Metallurgy: London, 1982; pp. 271−278.

(6) Fuerstenau, M. C. Sulphide Mineral Flotation. In *Principles of Flotation*; King, R. P., Ed.; SAIMM: Johannesburg, SA, 1982; pp. 159−182.

(7) Paulson, O.; Pugh, R. J. Flotation of Inherently Hydrophobic Particles in Aqueous Solutions of Inorganic Electrolytes. *Langmuir* **1996**, *12*, 4808−4813.

(8) Pugh, R. J.; Weissenborn, P.; Paulson, O. Flotation in Inorganic Electrolytes; the Relationship between Recover of Hydrophobic Particles, Surface Tension, Bubble Coalescence and Gas Solubility. *Int. J. Miner. Process.* **1997**, *51*, 125−138.

(9) Laskowski, J. S.; Liu, Q.; Bolin, N. J. Polysaccharides in Flotation of Sulphides. Part I. Adsorption of Polysaccharides onto Mineral Surfaces. *Int. J. Miner. Process.* **1991**, *33*, 223−234.

(10) Harvey, P. A.; Nguyen, A. V.; Evans, G. M. Influence of Electrical Double-Layer Interaction on Coal Flotation. *J. Colloid Interface Sci.* **2002**, *250*, 337−343.

(11) Laskowski, J.; Castro, S. Flotation in Concentrated Electrolyte Solutions. *Int. J. Miner. Process.* **2015**, *144*, 50−55.

(12) Li, C.; Somasundaran, P. Role of Electrical Double Layer Forces and Hydrophobicity in Coal Flotation in NaCl Solutions. *Energy Fuels* **1993**, *7*, 244−248.

(13) Wang, B.; Peng, Y. The Effect of Saline Water on Mineral Flotation − A Critical Review. *Miner. Eng.* **2014**, *66−68*, 13−24.

(14) Burdukova, E. *Surface Properties of New York Talc as a Function of PH, Polymer Adsorption and Electrolyte Concentration*. 2007.

(15) Ma, X.; Pawlik, M. Effect of Alkali Metal Cations on Adsorption of Guar Gum onto Quartz. *J. Colloid Interface Sci.* **2005**, *289*, 48−55.

(16) Manono, M. S.; Corin, K. C.; Wiese, J. G. The Influence of Electrolytes Present in Process Water on the Flotation Behaviour of a Cu-Ni Containing Ore. *Miner. Eng.* **2016**, 96−107.

(17) Manenzhe, R. M.; Corin, K. C.; Wiese, J. G.; Manono, M. S.; Musuku, B. The Effect of Water Quality on the Adsorption of a Xanthate Collector in the Flotation of a Sulphide Ore. In *IMPC 2018 - 29th International Mineral Processing Congress*; 2019.

https://doi.org/10.1021/acsomega.1c01152
ACS Omega 2021, 6, 28496−28506

(18) Manono, M. S.; Matibidi, K.; Thubakgale, C. K.; Corin, K. C.; Wiese, J. G. *Water Quality in PGM Ore Flotation : The Effect of Ionic Strength and PH*. 2017, 777−784.
(19) Becker, M.; De Villiers, J.; Bradshaw, D. The Flotation of Magnetic and Non-Magnetic Pyrrhotite from Selected Nickel Ore Deposits. *Miner. Eng.* **2010**, *23*, 1045−1052.
(20) Becker, M.; Harris, P. J.; Wiese, J. G.; Bradshaw, D. J. Mineralogical Characterisation of Naturally Floatable Gangue in Merensky Reef Ore Flotation. *Int. J. Miner. Process.* **2009**, *93*, 246−255.
(21) Qi, C.; Liu, J.; Malainey, J.; Kormos, L. J.; Coffin, J.; Deredin, C.; Liu, Q.; Fragomeni, D. The Role of Cu Ion Activation and Surface Oxidation for Polymorphic Pyrrhotite Flotation Performance in Strathcona Mill. *Miner. Eng.* **2019**, *134*, 87−96.
(22) Kelebek, S.; Tukel, C. Separation of Nickeliferous Hexagonal Pyrrhotite from Pentlandite in Ni-Cu Sulphide Ores: Recovery by Size Performance. *Miner. Eng.* **2018**, *125*, 223−230.
(23) Brough, C. P.; Bradshaw, D. J.; Becker, M. A Comparison of the Flotation Behaviour and the Effect of Copper Activation on Three Reef Types from the Merensky Reef at Northam. *Miner. Eng.* **2010**, *23*, 846−854.
(24) Chimbganda, T.; Becker, M.; Broadhurst, J. L.; Harrison, S. T. L.; Franzidis, J. P. A Comparison of Pyrrhotite Rejection and Passivation in Two Nickel Ores. *Miner. Eng.* **2013**, *46*−*47*, 38−44.
(25) Ekmeki, Z.; Becker, M.; Tekes, E. B.; Bradshaw, D. An Impedance Study of the Adsorption of CuSO4 and SIBX on Pyrrhotite Samples of Different Provenances. *Miner. Eng.* **2010**, *23*, 903−907.
(26) Ekmeki, Z.; Becker, M.; Tekes, E. B.; Bradshaw, D. The Relationship between the Electrochemical, Mineralogical and Flotation Characteristics of Pyrrhotite Samples from Different Ni Ores. *J. Electroanal. Chem.* **2010**, *647*, 133−143.
(27) Multani, R. S.; Waters, K. E. Flotation Recovery−by−Size Comparison of Pyrrhotite Superstructures with and without Depressants. *Miner. Eng.* **2019**, *130*, 92−100.
(28) Multani, R. S.; Waters, K. E. A Review of the Physicochemical Properties and Flotation of Pyrrhotite Superstructures (4C − Fe7S8/5C − Fe9S10) in Ni-Cu Sulphide Mineral Processing. *Can. J. Chem. Eng.* **2018**, *96*, 1185−1206.
(29) Multani, R. S.; Waters, K. E. Pyrrhotite Depression Studies with DETA and SMBS on a Ni-Cu Sulphide Ore. *Can. J. Chem. Eng.* **2019**, *97*, 2121−2130.
(30) Multani, R. S.; Williams, H.; Johnson, B.; Li, R.; Waters, K. E. The Effect of Superstructure on the Zeta Potential, Xanthate Adsorption, and Flotation Response of Pyrrhotite. *Colloids Surf., A* **2018**, *551*, 108−116.
(31) Allison, S. A.; O'Connor, C. T. An Investigation into the Flotation Behaviour of Pyrrhotite. *Int. J. Miner. Process.* **2011**, *98*, 202−207.
(32) Becker, M.; Brough, C. Geometallurgical Characterisation of the Merensky Reef at Northam Platinum Mine: Comparison of Normal Pothole and Transitional Reef Types. *9th International Congress for Applied Mineralogy* 2008, *79* (1989), 3−5.
(33) October, L.; Corin, K.; Schreithofer, N.; Manono, M.; Wiese, J. Water Quality Effects on Bubble-Particle Attachment of Pyrrhotite. *Miner. Eng.* **2019**, *131*, 230.
(34) Rao, S. R.; Finch, J. A. A Review of Water Re-Use in Flotation. *Miner. Eng.* **1989**, *2*, 65−85.
(35) Zanin, M.; Lambert, H.; du Plessis, C. A. Lime Use and Functionality in Sulphide Mineral Flotation: A Review. *Miner. Eng.* **2019**, *143*, No. 105922.
(36) Li, Y.; Li, W.; Xiao, Q.; He, N.; Ren, Z.; Lartey, C.; Gerson, A. The Influence of Common Monovalent and Divalent Chlorides on Chalcopyrite Flotation. *Minerals* **2017**, *7*, 111.
(37) Li, C.; Somasundaran, P. Reversal of Bubble Charge in Multivalent Inorganic Salt Solutions-Effect of Aluminum. *J. Colloid Interface Sci.* **1992**, *148*, 587−591.
(38) Ramos, O.; Castro, S.; Laskowski, J. S. Copper-Molybdenum Ores Flotation in Sea Water: Floatability and Frothability. *Miner. Eng.* **2013**, *53*, 108−112.
(39) Manono, M.; Corin, K.; Wiese, J. The Effect of the Ionic Strength of Process Water on the Interaction of Talc and CMC: Implications of Recirculated Water on Floatable Gangue Depression. *Minerals* **2019**, *9* (), DOI: 10.3390/min9040231.
(40) Niecikowska, A.; Krasowska, M.; Ralston, J.; Malysa, K. Role of Surface Charge and Hydrophobicity in the Three-Phase Contact Formation and Wetting Film Stability under Dynamic Conditions. *J. Phys. Chem. C* **2012**, *116*, 3071−3078.
(41) Stöckelhuber, K. W. Stability and Rupture of Aqueous Wetting Films. *Eur. Phys. J. E: Soft Matter Biol. Phys.* **2003**, *12*, 431−435.
(42) Zawala, J.; Karaguzel, C.; Wiertel, A.; Sahbaz, O.; Malysa, K. Kinetics of the Bubble Attachment and Quartz Flotation in Mixed Solutions of Cationic and Non-Ionic Surface-Active Substances. *Colloids Surf., A* **2017**, *523*, 118−126.
(43) Laskowski, J. S.; Liu, Q.; O'Connor, C. T. Current Understanding of the Mechanism of Polysaccharide Adsorption at the Mineral/Aqueous Solution Interface. *Int. J. Miner. Process.* **2007**, *84*, 59−68.
(44) Dishon, M.; Zohar, O.; Sivan, U. From Repulsion to Attraction and Back to Repulsion: The Effect of NaCl, KCl and CsCl on the Force between Silica Surfaces in Aqueous Solution. *Langmuir* **2009**, *25*, 2831−2836.
(45) Hirajima, T.; Suyantara, G. P. W.; Ichikawa, O.; Elmahdy, A. M.; Miki, H.; Sasaki, K. Effect of Mg2+ and Ca2+ as Divalent Seawater Cations on the Floatability of Molybdenite and Chalcopyrite. *Miner. Eng.* **2016**, *96*−*97*, 83−93.
(46) Blake, T. D.; Kitchener, J. A. Stability of Aqueous Films on Hydrophobic Methylated Silica. *J. Chem. Soc., Faraday Trans. 1* **1972**, *68*, 1435−1442.
(47) Craig, V. S. J.; Ninham, B. W.; Pashley, R. M. The Effect of Electrolytes on Bubble Coalescence in Water. *J. Phys. Chem.* **1993**, *97*, 10192−10197.
(48) Moignard, M. S.; James, R. O.; Healy, T. W. Adsorption of Calcium at the Zinc Sulphide-Water Interface. *Aust. J. Chem.* **1977**, *30*, 733−740.
(49) Wang, T.; Liu, G.; Zhang, G.; Craig, V. S. J. Insights into Ion Specificity in Water-Methanol Mixtures via the Reentrant Behavior of Polymer. *Langmuir* **2012**, *28*, 1893−1899.
(50) Ikumapayi, F.; Makitalo, M.; Johansson, B.; Rao, K. H. Recycling of Process Water in Sulphide Flotation: Effect of Calcium and Sulphate Ions on Flotation of Galena. *Miner. Eng.* **2012**, *39*, 77−88.
(51) Kirjavainen, V.; Schreithofer, N.; Heiskanen, K. Effect of Calcium and Thiosulfate Ions on Flotation Selectivity of Nickel-Copper Ores. *Miner. Eng.* **2002**, *15*, 1−5.
(52) Takahashi, M. ζ Potential of Microbubbles in Aqueous Solutions: Electrical Properties of the Gas - Water Interface. *J. Phys. Chem. B* **2005**, *109*, 21858−21864.
(53) Lessard, R. R.; Zieminski, A. S. Bubble Coalescence and Gas Transfer in Aqueous Electrolytic Solutions. *Ind. Eng. Chem. Fundam.* **1971**, *10*, 260−269.
(54) Craig, V. S. J. Bubble Coalescence and Specific-Ion Effects. *Curr. Opin. Colloid Interface Sci.* **2004**, *9*, 178−184.
(55) Manono, M.; Corin, K. Determining the Ions with the Most Impact on Froth Stability in Cu-Ni-PGM Ore Flotation. In *Proceedings of the XXX International Mineral Processing Congress, Cape Town, South Africa, 18−22 April 2022*; Cape Town, 2020.
(56) Wiese, J.; Harris, P.; Bradshaw, D. The Influence of the Reagent Suite on the Flotation of Ores from the Merensky Reef. *Miner. Eng.* **2005**, *18*, 189−198.
(57) Corin, K. C.; Reddy, A.; Miyen, L.; Wiese, J. G.; Harris, P. J. The Effect of Ionic Strength of Plant Water on Valuable Mineral and Gangue Recovery in a Platinum Bearing Ore from the Merensky Reef. *Miner. Eng.* **2011**, *24*, 131−137.
(58) Manono, M.; Corin, K.; Wiese, J. Water Quality Effects on a Sulfidic PGM Ore : Implications for Froth Stability and Gangue

https://doi.org/10.1021/acsomega.1c01152
ACS Omega 2021, 6, 28496−28506

Management. *Physicochem. Probl. Miner. Process* **2018**, *54*, 1253−1265.
(59) Yoon, R. H.; Yordan, J. L. Induction Time Measurements for the Quartz-Amine Flotation System. *J. Colloid Interface Sci.* **1991**, *141*, 374−383.
(60) Jávor, Z.; Schreithofer, N.; Heiskanen, K. Multi-Scale Analysis of the Effect of Surfactants on Bubble Properties. *Miner. Eng.* **2016**, *99*, 170−178.
(61) Javor, Z., Aspiala, M., Schreithofer, N., Heiskanen, K., Serna, R. Development of a New Attachment Timer for Predicting the Change in Ore Floatability. In *Proceedings of the XXVIII International Mineral Processing Congress (IMPC 2016), September 11-15, 2016*, Canadian Institute of Mining, Metallurgy and Petroleum: Québec City; 2016.
(62) Aspiala, M.; Schreithofer, N.; Serna-Guerrero, R. Automated Contact Time Apparatus and Measurement Procedure for Bubble-Particle Interaction Analysis. *Miner. Eng.* **2018**, *121*, 77−82.
(63) Bradshaw, D. J.; Connor, C. T. Measurement of the Sub-Process of Bubble Loading in Flotation. *Miner. Eng.* **1996**, *9*, 443−448.
(64) Wang, X.; Liu, R.; Ma, L.; Qin, W.; Jiao, F. Depression Mechanism of the Zinc Sulfate and Sodium Carbonate Combined Inhibitor on Talc. *Colloids Surf., A* **2016**, *501*, 92−97.

https://doi.org/10.1021/acsomega.1c01152
ACS Omega 2021, 6, 28496−28506